Available online at www.sciencedirect.com
SCIENCE DIRECT®
Journal of Sound and Vibration 286 (2005) 645–652
JOURNAL OF SOUND AND VIBRATION
www.elsevier.com/locate/jsvi

Application of chaos method to line spectra reduction

Jing-jun Lou*, Shi-jian Zhu, Lin He, Xiang Yu

Institute of Noise & Vibration, Naval University of Engineering, Wuhan 430033, PR China

Received 29 September 2004; accepted 16 December 2004
Available online 8 March 2005

1. Introduction

The spectra of the radiated waterborne-noises of marine vessels are generally in two categories. One is broad-band noise having a continuous spectrum. The other is line spectrum. The total radiated signature is usually a combination of broad-band and line spectra. The nature of the radiated noise spectra changes as the navigation speed changes. At high speed, the signature is dominated by broad-band noise, while at low speed the signature is dominated by line spectra, and the machinery is the leading noisemaker.

Insertion of resilient isolators between the machinery and the base is one of the most common methods for controlling unwanted vibration. The isolators in service are usually assumed to be linear and almost all the vibration isolation systems are designed with linear theory. The linear vibration isolation system has vibration attenuation within a rather wide frequency range. But its ability in line spectra reduction is limited. The superposition principle and frequency conservation are the primary characteristics of the linear system. Namely, for sinusoidal input, the output is also sinusoidal with the same frequency and therefore, the linear vibration isolation cannot change the frequency spectra configuration of the radiated waterborne noise.

For the deficiency of the linear vibration isolators, nonlinear isolators were studied in some literatures. However, the investigation was constrained to the periodic vibration. For example, with the method of harmonic balance, B. Ravindra analyzed the harmonic response of a cubic nonlinear vibration isolation system [1] and the performance of vibration isolators with nonlinearity in both stiffness and damping under harmonic excitations [2].

*Corresponding author. Tel.: +86 27 83443233; fax: +86 27 83443990.
E-mail address: jingjun_lou@hotmail.com (J.-j. Lou).

0022-460X/$ - see front matter
doi:10.1016/j.jsv.2004.12.018

Since Ueda's [3] work on Duffing's equation, it is well known that nonlinear vibration systems under harmonic excitation can exhibit chaotic responses [4–6]. However, the investigation on the mechanism of chaos, rather than the study of isolation characteristic or the application of chaos in vibration isolation, seems to be the main objective of the work in Refs. [4–6]. In spite of the achievement in the application of the chaotic vibration mechanics to chaotic vibratory rollers [7], it is neglected that vibration excitation and vibration isolation are two poles of vibration and no efforts are made to make use of chaos in vibration isolation. The author tries to utilize the characteristics of chaos to vibration isolation and a method of chaotic vibration isolation is advanced for machinery vibration control and line spectra reduction. When chaos takes place in a vibration isolation system with nonlinear isolator, the line spectra grow into a broad-band one. Therefore, the frequency configuration of the radiated noise is altered. What is more important, the concentrated energy spreads from the excitation frequency to a broad-band frequency range.

2. Route to chaos and scaling property of the power spectrum

As is known, nonlinear oscillating systems subject to external excitation can exhibit complex regular behavior. The classical regular response includes primary, super-, sub-, ultrasubharmonic resonances. These deterministic systems can also exhibit chaos, i.e. apparently random behavior with extremely sensitive dependence on initial conditions. A very simple looking continuous dynamical system, which nevertheless exhibits all these phenomena, is the Duffing system

$$\ddot{x} + \delta\dot{x} + x + x^3 = f\cos\omega t. \tag{1}$$

The eigenfrequency Ω of the Duffing system (1) depends on the excitation amplitude f and two asymptotically orbitally stable solutions may coexist for a certain range of the excitation frequency ω. These properties lead to the well-known leaning over of the amplitude resonance curve and to hysteresis jumps.

Every periodic solution $x(t)$ of (1) can be expanded into Fourier series

$$x(t) = \sum_x x_k e^{ik\omega t}. \tag{2}$$

Duffing system (1) is a symmetrical one respect to x, that is, it preserves the form under the transformation of $x \to -x$, $t \to \pi/\omega + t$. For sufficiently small excitations the solution of (1) should be also symmetrical. All Fourier coefficients x_k in the Fourier series (2) do not vanish for odd $k \in Z$ and coefficients with even k are all equal to zero. For excitation frequencies ω below the main resonance we therefore have a secondary resonance, whenever $k\omega$ equals the amplitude dependent eigenfrequency Ω of the system. And x_k is called the superharmonic response.

If the excitation amplitude f is high enough the closed trajectory may lose its geometrical symmetry. This is the so-called symmetry breaking bifurcation, caused by the non-zero of the even Fourier coefficients. The symmetry breaking bifurcation may therefore be viewed as resonances $\omega = \Omega/k$ for even $k \in Z$.

Parlitz [8] demonstrated that cascades of period-doubling bifurcation take place in the parameter region, where the orbits have lost their symmetry. It can easily be shown that even subharmonics, i.e. subharmonics whose period equals an even multiple of the excitation period,

obtained from period-doubling bifurcations are always asymmetrical. Symmetry breaking is therefore a prerequisite for period-doubling bifurcations. Further increase of the excitation amplitude f, the period-doubling bifurcations accumulate and a sequence of chaotic attractors appears.

For periodic solutions whose periods are equal to 2^nT, where $n = 0, 1, 2,\ldots$ and $T = 2\pi/\omega$ is the excitation period, the power spectrum $P(\omega)$ is a series of impulse function at frequencies $\omega' = m\omega/2^n$ where $m = 1, 2,\ldots 2^n$. Comparing the spectral lines in $P(\omega)$, we find that a new spectral line in $P(\omega)$ of the periodic $2^{n+1}T$ solution bursts out between every two adjacent lines of the periodic 2^nT solution, that is, some new frequencies of $\omega' = (2m-1)\omega/2^{n+1}$ come forth in the periodic $2^{n+1}T$ solution. For the sake of calculation of the strength of spectral lines from period-doubling bifurcation, $P(\omega)$ can be written as

$$P(\omega) = \sum_{n=0}^{\infty}\sum_{m=1}^{2^{n-1}} P_{n,m}\delta\left(\frac{2m-1}{2^n}\omega\right), \tag{3}$$

where $P_{n,\,m}$ is the strength of the mth spectral line from the nth period-doubling bifurcation.

Let

$$P(n) \equiv \frac{1}{2^{n-1}}\sum_{m=1}^{2^{n-1}} P_{n,m} \tag{4}$$

denotes the mean strength of the spectral lines from the nth period-doubling bifurcation, and get [9]

$$10\,\log\frac{P(n)}{P(n+1)} = 13.21\,\text{dB}. \tag{5}$$

Eq. (5) indicates the descending of the power spectrum in the cascades of period-doubling bifurcation, as shown in Fig. 1, where the distances between every two adjacent dashed lines are equivalent. The new spectral lines from once period-doubling bifurcation is 13.21 dB less than that from the previous bifurcation. The deeper the period-doubling bifurcation, the lower the power

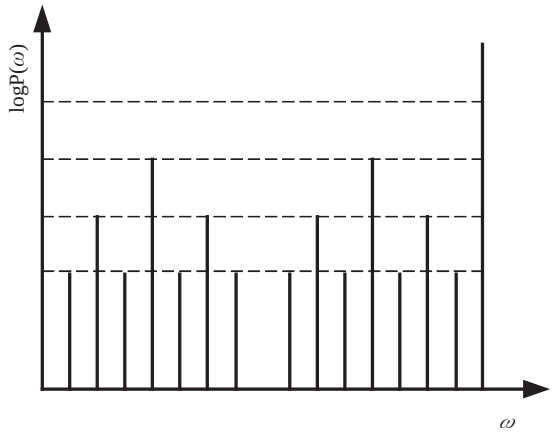

Fig. 1. Scaling property of the power spectra in the cascades of period-doubling bifurcations.

spectrum and the more new frequencies appear. The period-doubling bifurcations accumulate until chaos appears. By now n is very large, the peak values of the spectrum fall a lot, and the power spectrum becomes continuous. The spectral broadening and spectral drop are hallmarks of the onset of chaos. If the desired chaos in the nonlinear vibration isolation system is gained, the line spectra reduction efficiency will be enhanced. From the viewpoint of energy, originally centralized energy is distributed to a broad-band frequency range.

3. Chaotic vibration isolation and performance index

Frequency conservation is the main characteristics of the linear system, so for the linear vibration isolation system with external sinusoidal excitation the energy transmitted to the base via the linear isolator will still concentrate on the excitation frequency. The nonlinear oscillating systems subject to external harmonic excitation can exhibit a great variety of harmonic responses, even countless when chaos appears. The concentrated energy therefore spreads from the frequency of excitation to a broad-band frequency range. For the given input energy into the vibration isolation system, the response energy at the excitation frequency for the chaotic vibration isolation system is much less than that for the linear vibration isolation system. So the chaos method is a good candidate for the line spectrum reduction.

The approaches for the chaos method in eliminating the line spectrum are as follows:

(1) Build the dynamics model for the nonlinear vibration isolation system with respect to the nonlinear isolator, and determine the numeric area of the stiffness and damping where the desired chaos appears.
(2) Determine the technically feasible approach to control the stiffness and damping to the chaotic parameter area.
(3) Chaos is realized and the line spectrum is suppressed.

For a linear vibration isolation system the force transmissibility is used to evaluate the effectiveness of vibration isolation. In a nonlinear system, however, a harmonic response with the same frequency as that of the excitation is not guaranteed. The response may contain subharmonics and superharmonics, and sometimes the response may even be chaotic. Hence, the force transmissibility makes no sense in the nonlinear vibration system and the problem of defining a suitable performance index for the nonlinear isolator is encountered. A working index defined as the ratio of the rms values of the response vs. the excitation may be used:

$$T = \sqrt{E[y^2]} \Big/ \sqrt{E[x^2]}, \tag{6}$$

where $E[x^2]$ and $E[y^2]$ denote the rms values of the excitation and response, respectively. This index shows the energy transmission relationship and it is easy to calculate and measure.

Expressed with decibel, Eq. (6) becomes

$$L = 20 \log \frac{\mathrm{RMS}(y)}{\mathrm{RMS}(x)}, \tag{7}$$

where $\mathrm{RMS}(\cdot) = \sqrt{E[\cdot^2]}$. In practice, the acceleration is easy to measure. Therefore, x and y are the acceleration at the upside and bottom of the isolator, respectively. L in Eq. (7) then becomes the drop of the acceleration vibration level.

This working index can evaluate the overall vibration isolation performance, however, it is devoid of any information about the response frequency content and cannot indicate the weakening of the line spectrum. One of the most advantages of the chaotic vibration isolation lies in isolating the line spectrum. To indicate the reduction of the line spectrum, another index, the difference between the power spectra of the response and the excitation at the excitation frequency, should be used.

4. Experiment

To validate the effectiveness of the method of chaotic vibration isolation, an experiment system is designed. The vibration excitor in the experiment is shown in Fig. 2. The motor 1 and gear wheels 2 drive the eccentric blocks 4 to reverse rotary. The excitation forces in the horizontal direction are balanced, leaving only the vertical force. The vibration excitor is supported by 4 pieces of hard Duffing-type vibration isolators whose stiffness can be adjusted through charge and blowoff. The experimental data is collected and analyzed with the Pimento Data Collecting System from the LMS Company. On both the upside and bottom of each isolator are accelerator sensors. Through the change of the revolution speed of the motor, the mass of the eccentric blocks, and the eccentricity, the excitation amplitude and frequency can be adjusted. The acceleration spectrogram is observed for real time. If the spectrogram is continuous, it should be initially estimated that chaos might occur. Further analysis of the time-series data, including phase space reconstruction, the maximal Lyapunov exponent, and the fractal dimension, can exactly judge whether the system is chaotic or not.

Fig. 3 shows the bifurcation diagram for the rotate speed $n = 1260\,\mathrm{rev/min}$, namely, the excitation frequency $\omega = 21\,\mathrm{Hz}$. To obtain the diagram the excitation amplitude f has been increased from 0 to 25 N and the Poincaré map of the response is plotted. A Poincaré map is

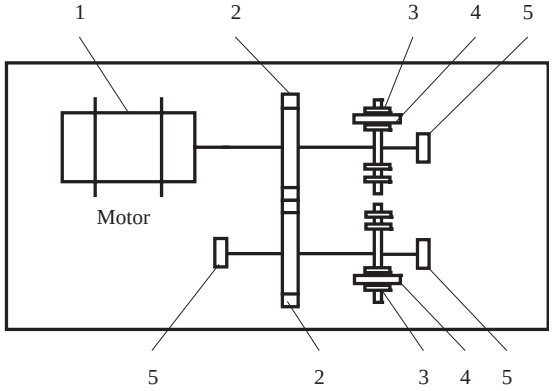

Fig. 2. Vertical vibration excitor: 1, motor; 2, gear wheel; 3, locknut; 4, eccentric block; 5, bearing.

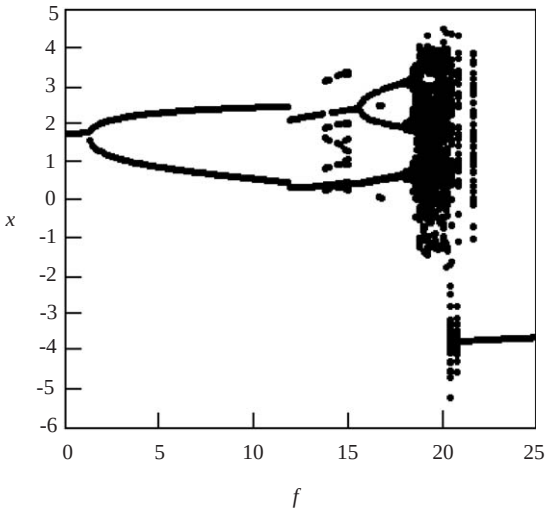

Fig. 3. Bifurcation diagram.

simply a stroboscopic phase plane plot that only records those phase points at intervals of a forcing period. The Poincaré map of an NT ($T = 2\pi/\omega$) response is N points.

Two cascades of period-doubling bifurcations are observed before the chaos occurs, as shown in Fig. 3. When $f < 1.2$ N, the response has the same period as that of the excitation, namely, period $1T$ solution. When $f = 1.2$ N, a response of period $2T$ is observed after once period-doubling bifurcation. Unlike the classical nonlinear system in numerical simulation, however, this period-doubling bifurcation does not accelerate as the excitation amplitude increases, and instead it is broken by another cascade of period-doubling bifurcation which originates from a $6T$ periodic response at $f = 13.6$ N. Then it becomes a response of period $12T$ at $f = 14.7$ N. Thereafter, the first period-doubling bifurcation comes back at $f = 15.1$ N where the response is of period $2T$. Further increase of the excitation amplitude f leads to deeper bifurcation cascades, responses of period $4T$ and $8T$ at $f = 15.6$ N and 17.8 N, respectively. Further cascades of period-doubling bifurcations do not take place and chaos occurs when $18.3 < f < 21.9$. Finally, the system rests on period $1T$ motion.

Fig. 4(a) is the spectrogram of the acceleration from the upside and bottom of one isolator when $f = 20$ N and $\omega = 21$ Hz. In spite of some sharp spectral lines there are many continuous part of the spectrum. It is very likely that chaos has occurred. To verify the onset of chaos, delay reconstruction is established, and the reconstructed attractors are shown in Fig. 5(a) and (b). We can see the apparent "strange" characteristic in the reconstructed attractors. Because of the stretch and folding, the attractors have infinite cascades of self-similarity. Lyapunov exponents have proven to be the most useful dynamical diagnostic for chaos. With the algorithm proposed by Wolf [10], the maximal Lyapunov exponents of the two reconstructed attractors in Fig. 5 are estimated 1.4308 and 0.8276, respectively. We can conclude that the motion of the system is chaotic. Fig. 4(b) is the spectrogram of the acceleration from the upside and bottom of one isolator when $f = 16$ N and $\omega = 20$ Hz. The spectral lines are apparent at the excitation frequency. Further data analysis demonstrates that the motion of the system is periodic.

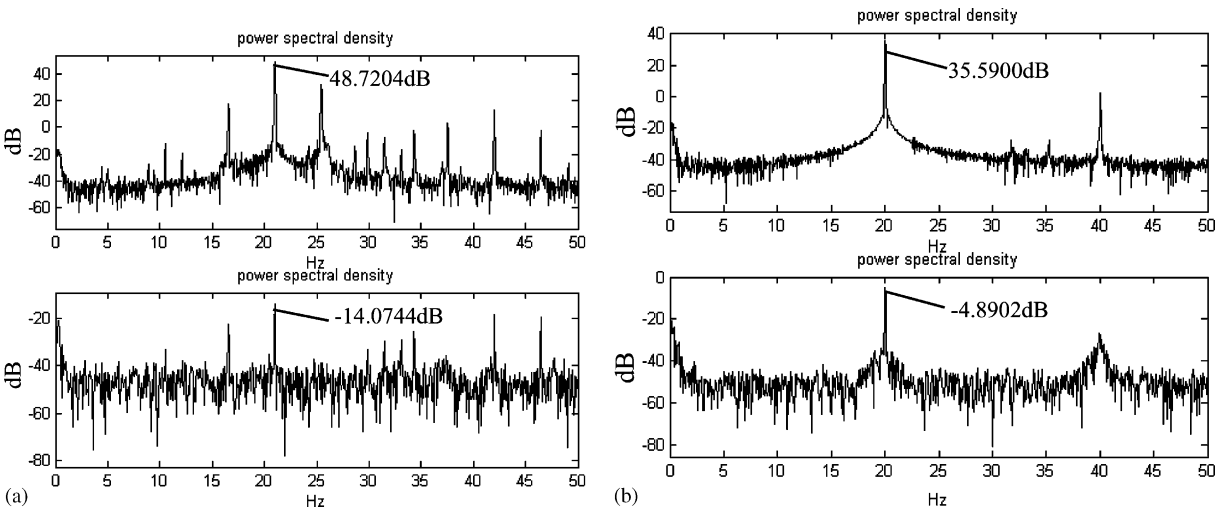

Fig. 4. Spectrogram of the acceleration from the upside and bottom of the isolator: (a) chaotic; (b) non-chaotic.

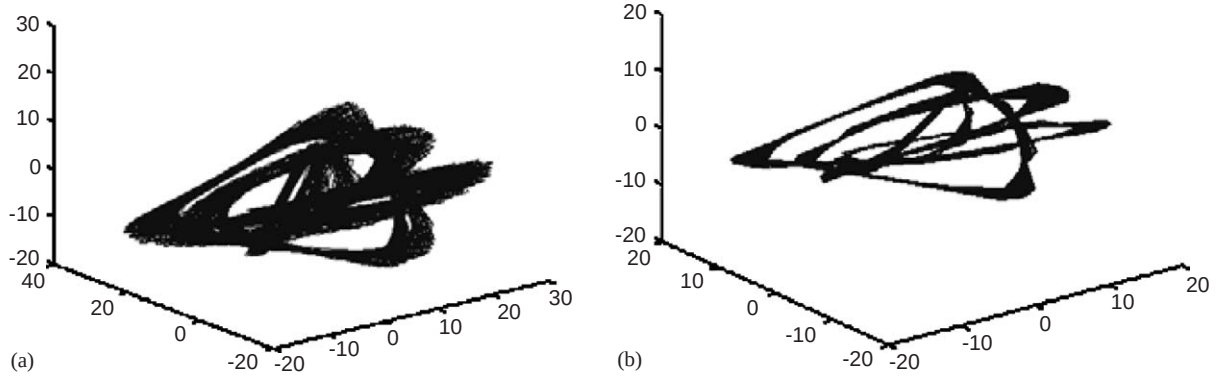

Fig. 5. Reconstructed strange attractors: (a) acceleration from the upside of the isolator; (b) acceleration from the bottom of the isolator.

As shown in Fig. 4(a), the power spectrum of the accelerator from the upside of the isolator at the excitation frequency of 21 Hz is 48.7204 dB, and that from the bottom of the isolator is −14.0744 dB. The drop in level is 62.7948 dB. In Fig. 4(b), the power spectrum of the accelerator from the upside of the isolator at the excitation frequency of 20 Hz is 35.5900 dB, and that from the bottom of the isolator is –4.8902 dB. The fall is 40.4802 dB. Thus, it can be seen that the reduction of the line spectra when the system is chaotic is much greater than that when the system is non-chaotic.

In terms of Eq. (7), the drop of the acceleration vibration level is 57.4369 dB when $f = 20$ N and $\omega = 21$ Hz, and 39.9486 dB when $f = 16$ N and $\omega = 20$ Hz. This shows that the overall effectiveness of vibration isolation at chaos is also better than that at non-chaos.

5. Conclusion

For the sake of reduction of line spectra in the radiated acoustical signature of marine vessels, the method of chaotic vibration isolation is advanced. This work is one of the few efforts to apply the chaos in engineering. Starting with the route to chaos and the scaling property of the power spectrum in the cascade of period-doubling bifurcations, the principle of the method of chaotic vibration isolation is derived. Two performance indices for the method presented in this paper, the ratio of the rms values of the response vs. the excitation and the difference of the power spectra between the response and the excitation at the frequency of line spectra, are also given. The presented method is experimentally verified. Experiment results show that the reduction of the line spectra when the system is chaotic is much greater than that when the system is non-chaotic, and that the overall effectiveness of vibration isolation at chaos is better than that at non-chaos.

References

[1] B. Ravindra, A.K. Mallik, Hard Duffing-type vibration isolator with combined Coulomb and viscous damping, *International Journal of Non-linear Mechanics* 28 (1993) 427–440.
[2] B. Ravindra, A.K. Mallik, Performance of non-linear vibration isolation under harmonic excitation, *Journal of Sound and Vibration* 170 (1994) 325–337.
[3] Y. Ueda, Explosions of strange attractors exhibited by Duffing's equation, *Annals of the New York Academy of Sciences* 357 (1980) 422–433.
[4] S. Novak, R.G. Frehlich, Transition to chaos in the Duffing oscillator, *Physical Review A* 26 (1982) 3660–3663.
[5] T. Fang, E.H. Dowell, Numerical simulations of periodic and chaotic responses in a stable Duffing system, *International Journal of Non-linear Mechanics* 22 (1987) 401–425.
[6] W. Szemplinska-Stupnicka, Secondary resonances and approximate models of routes to chaotic motion in non-linear oscillators, *Journal of Sound and Vibration* 113 (1987) 155–172.
[7] Long Yunjia, Wang Congling, Zhang Ping, Road roller based on chaotic theory, *Journal of China Agricultural University* 3 (1998) 19–22.
[8] Ulrich Parlitz, Werner Lauterborn, Superstructure in the bifurcation set of the Duffing equation, *Physics Letters A* 107 (1985) 351–355.
[9] Chen Shigan, *Maps and Chaos*, Press of National Defence Industry, Beijing, 1992.
[10] A. Wolf, J.B. Swift, Determining Lyapunov exponents from a time series, *Physica D* 16 (1985) 285–317.